Catal Lett (2015) 145:220–232
DOI 10.1007/s10562-014-1400-8

Surface Chemistry for Enantioselective Catalysis

Andrew J. Gellman · Wilfred T. Tysoe · Francisco Zaera

Received: 6 October 2014 / Accepted: 10 October 2014 / Published online: 16 October 2014

Abstract A Perspective is offered on the lessons learned from surface-science studies on enantioselective chemistry on solid surfaces performed by the author's groups. Our emphasis is on studies on model systems, mainly metal single-crystal surfaces under controlled environments, but extension of such research to more realistic samples relevant to heterogeneous catalysis is also briefly discussed. Enantioselective chemistry on surfaces is here divided into three guiding modalities, depending on the underlying mechanism. First, enantioselective chemistry resulting from the use of intrinsically chiral surfaces, which can be made from achiral solids such as metals by exposing the appropriate planes, is discussed. Next, the imparting of enantioselectivity to achiral surfaces by modifying them with adsorbates is classified in terms of two operating mechanisms: first, via the formation of supramolecular surface ensembles with chiral adsorption sites, and second, by relying on the effect of the local chiral environment intrinsically provided by the chiral modifiers through a one-to-one interaction between the modifier and the reactant. A discussion is then provided on studies with more complex samples involving metal nanoparticles and high-surface-area porous oxides. Finally, the present state of our understanding of enantioselective surface chemistry and the prognosis for the future are provided.

Keywords Chiral · Enantioselectivity · Templating · Surface science · Catalysis

A. J. Gellman
Department of Chemical Engineering, Carnegie Mellon University, Pittsburgh, PA 15213, USA

W. T. Tysoe
Department of Chemistry and Biochemistry and Laboratory for Surface Studies, University of Wisconsin-Milwaukee, Milwaukee, WI 53211, USA

F. Zaera (✉)
Department of Chemistry, University of California-Riverside, Riverside, CA 92521, USA
e-mail: zaera@ucr.edu; francisco.zaera@ucr.edu

1 Introduction

While much of the early work in catalysis focused on improving activity, defined as the rate at which reactants are converted into products, more recently the emphasis has shifted to improving selectivity, to make more effective use of the reactants and to minimize waste products [1–3]. Enantioselectivity, in which one enantiomer of a chiral product is formed in favor of the other, is perhaps the subtlest and most difficult-to-control example of selectivity: in a chiral compound, the two enantiomers (typically denoted *R* and *S*, or sometimes D- and L-) are identical except for the stereographic arrangement of their atoms, which generates enantiomer pairs that are not superimposable on one another. Enantiomers exhibit identical chemical behavior except when reacting with other enantiomerically pure chiral compounds. Since much of the biochemistry of living organisms relies on single enantiomers of chiral compounds, enantioselectivity has acquired increasing relevance in those industries producing or using bioactive chemicals.

Indeed, from a practical point of view, controlling enantioselectivity in catalysis is critical to the synthesis of chiral pharmaceutical and agrochemical compounds [4, 5]. Many pharmaceuticals are currently synthesized by homogeneous-phase catalysts, and those, in many instances, are non-enantioselective. Moreover, homogeneous processes require subsequent steps for the separation of

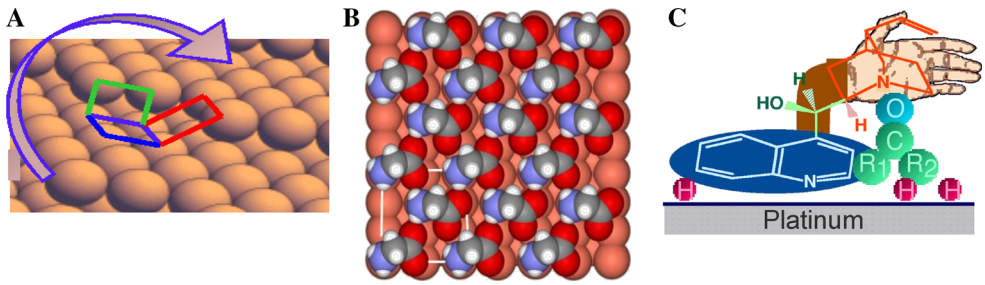

Fig. 1 Illustration of the three modalities described in this Perspective for the bestowing of enantioselectivity to solid surfaces. **a** A naturally chiral surface exposes a crystalline atomic structure that lacks mirror symmetry and thus is chiral. **b** An ordered array of chiral or prochiral adsorbates forms a template that lacks mirror symmetry and therefore imparts chirality to the surface. **c** Isolated chiral adsorbates interact enantiospecifically with individual chiral or prochiral molecules

products from catalysts. The development of enantioselective heterogeneous catalysts for the production of chiral pharmaceuticals would eliminate the large amounts of waste generated with current methods, making the process greener, would reduce the cost incurred in the production of chiral compounds as racemic mixtures and their subsequent separation into enantiomerically pure components, and would also eliminate the difficulties associated with the separation of the catalyst from the final product.

There have been significant efforts to develop such heterogeneous-phase catalytic systems by trial-and-error methods, but those have so far shown only limited success, yielding large enantiomeric excesses (ee's) almost exclusively in hydrogenation reactions with selected α- and β-ketoesters [6–8]. There is a need to develop a fundamental understanding of the principles that underpin enantioselective catalysis in order to be able to design and develop new chiral catalyst systems. Since the central chemistry controlling heterogeneous catalysis occurs at the interface between gases or liquids and the solid surfaces used as catalysts, advances in enantioselective heterogeneous catalysis at a molecular level requires a focus on understanding chiral surface chemistry. During the past decade, our three research groups have been working in a coordinated way to contribute to the advancement of this area. In this Perspective, we discuss the main lessons learned so far from that effort.

Enantioselective catalysis arises from enantiospecific interactions of prochiral and chiral species (adsorbed reactants, intermediates, transition states, or products) with chiral catalytic surfaces. These interactions manifest themselves as differences in energetics between *R*- and *S*-chiral adsorbates on the *R*- (or *S*-) enantiomorphs of the catalyst. The mechanisms by which these interactions are affected by chirality may be roughly categorized into three types (Fig. 1) [9–12]:

- *Naturally chiral surfaces*, where surfaces have intrinsically chiral atomic structures (Fig. 1a). Chiral bulk materials such as quartz or calcite inherently expose chiral surfaces, but achiral bulk structures can also expose chiral surfaces in some instances. In fact, the majority of the high-Miller index surfaces of single crystals are chiral [13]. Interactions of chiral adsorbates with naturally chiral surfaces are enantiospecific.
- *Chirally templated surfaces*, where molecules adsorbed on achiral surfaces self-assemble into ordered chiral structures with long-range periodicity (Fig. 1b). Imparting chirality in this way is expected for chiral molecules, but can in fact also occur for molecules that are not chiral in the gas phase as long as adsorption of such prochiral molecules removes their mirror plane of symmetry (although, in the absence of a chiral symmetry, they would form equal amounts of left- and right-handed domains).
- *One-to-one chiral modifiers*, where an isolated chiral modifier on an achiral surface interacts enantiospecifically with a prochiral adsorbate to form a one-to-one complex, orienting the adsorbate enantiospecifically upon adsorption on the surface (Fig. 1c). Such a one-to-one interaction does not require the modifier to form an ordered array on the surface, although this may still happen. In this classification, the dominant interaction in one-to-one modification is between a prochiral molecule and the chiral modifier.

While these categorizations are, to some extent, artificial, and while a particular modifier may operate by a mixture of two or more of these types of interaction, the division described above represents a useful conceptual framework for organizing this Perspective. In the following sections we discuss some of the recent advances coming from our laboratories on the understanding of these three modalities of surface enantioselectivity. The focus is on work using model systems, typically single-crystal surfaces under ultrahigh vacuum (UHV) conditions, but some data are also reported from our recent studies with more realistic catalytic samples and conditions. The emphasis of this

review is on the contribution to the field by the authors, but reference is also made to some of the key reports from other groups.

2 Naturally Chiral Surfaces

It was realized some time ago that high-Miller-index surfaces of single crystalline materials consisting of kinked steps separated by flat low Miller index terraces are intrinsically chiral [12, 14–16]. These surfaces are therefore expected to exhibit enantioselective surface chemistry. In their original work articulating these ideas, Gellman and coworkers used a chiral molecule, 2-butanol, to probe such enantioselective behavior on $Ag(643)^R$ versus $Ag(643)^S$ single-crystal surfaces [16]. Although no detectable differences in adsorption energetics or in the kinetics of dehydrogenation reactions could be seen by temperature programmed desorption (TPD) between homochiral (*R*-2-butanol on $Ag(643)^R$ and *S*-2-butanol on $Ag(643)^S$) and heterochiral (*R*-2-butanol on $Ag(643)^S$ and *S*-2-butanol on $Ag(643)^R$) pairs of reactants and surfaces, later work with similar systems did show clear enantiospecific differences in reaction energetics. Indeed, Sholl et al., based on quantum mechanics calculations, predicted that chiral molecules such as trans-1,2-dimethylcycloalkanes and limonene should display enantiospecific differences in adsorption energies on $Pt(643)^{R\&S}$ of up to 2 kcal/mole [17, 18]. Subsequent experimental studies on the electro-oxidation of D- and L-glucose on chiral $Pt(643)^{R\&S}$ and $Pt(531)^{R\&S}$ surfaces revealed differences in the rate of oxidation of as much as a factor of 3 depending upon the handedness of the reactant with respect to that of the surface [19, 20].

Since then, Gellman et al. have reported results on a number of systems where these enantiospecific differences in reaction energetics have been clearly detected. The first example was that of *R*-3-methyl-cyclohexanone (*R*-3-MCHO), for which a difference in desorption energy at the kink sites of $\Delta(\Delta E_{des}) = 1.0 \pm 0.2$ kJ/mole was measured between the $Cu(643)^R$ and $Cu(643)^S$ surfaces (Fig. 2) [21]. Other chiral molecules, including propylene oxide [22, 23], lysine [24], and several bromoalkanes [25, 26], were later shown to exhibit comparable enantioselective energetic differences on these and other Cu chiral surfaces [27–29]. Enantiospecific differences in adsorption energetics between enantiomers on a chiral surface must be accompanied by enantiospecific differences in adsorbate geometry and orientation. These can be detected using Fourier Transform Infrared Reflection Absorption Spectrometry (FT-IRAS) as difference in the relative intensities of absorption bands. As examples, the orientations of *R*- and *S*-2-butanoxy groups have been shown to differ on the $Ag(643)^R$ surface [21] and the orientations of *R*-3-MCHO

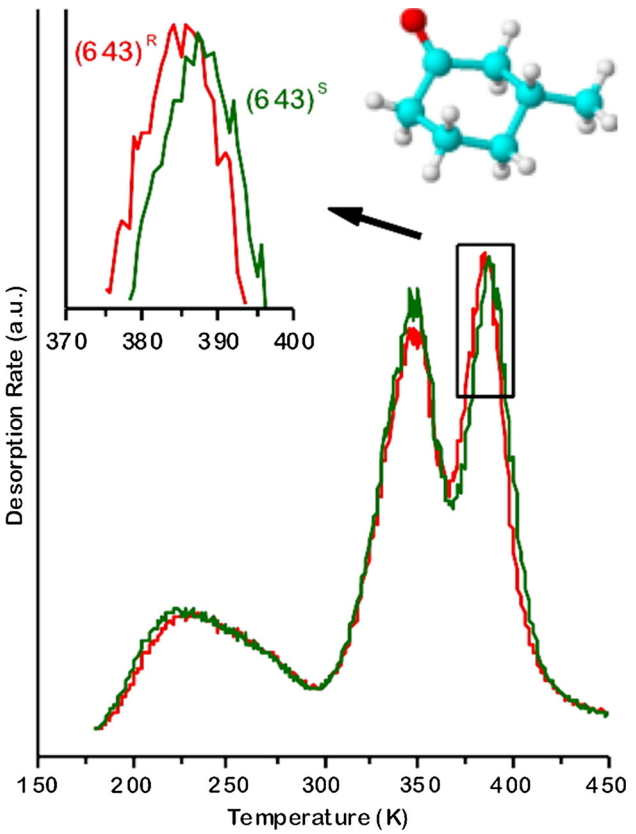

Fig. 2 Contrasting TPD traces from *R*-3-methylcyclohexanone adsorbed on $Cu(643)^R$ (*red trace*) versus $Cu(643)^S$ (*green*) surfaces. The shift in desorption peak maximum, by 3.5 K, from the $Cu(643)^S$ surface relative to the $Cu(643)^R$ surface, is clearly seen in the magnified view of the high-temperature peak shown in the inset, indicating an energetic differences between the homochiral and heterochiral adsorbate–surface pairs. Reproduced from Ref. [23, Fig. 4] with permission, Copyright 2002 The American Chemical Society

have been shown to be enantiospecific in the $Cu(643)^{R\&S}$ surfaces [30]. A systematic study of the enantioselectivity of the adsorption of *R*-3MCHO at the kink sites on seven different chiral Cu surfaces has shown that enantiospecific adsorption is observed at the kink sites on these surfaces, that the enantiospecificity of the adsorption energetics is in the range 0.6–1.1 kJ/mole, and that the sign of the energy difference can vary across Cu crystal planes [21, 23, 27–29].

In all the studies mentioned above, it has been shown that enantiospecific differences in the interaction energies of chiral molecules with chiral surfaces are small and typically lead to modest enantioselectivities in adsorption, catalysis, and chemistry on chiral surfaces. To yield high enantioselectivities, those small energy differences must be amplified by non-linear processes. Exploitation of small differences in adsorption equilibria for the enantiopurification of racemic mixtures of chiral compounds may be envisioned. The first demonstration of an enantiospecific separation on a naturally chiral surface used the small

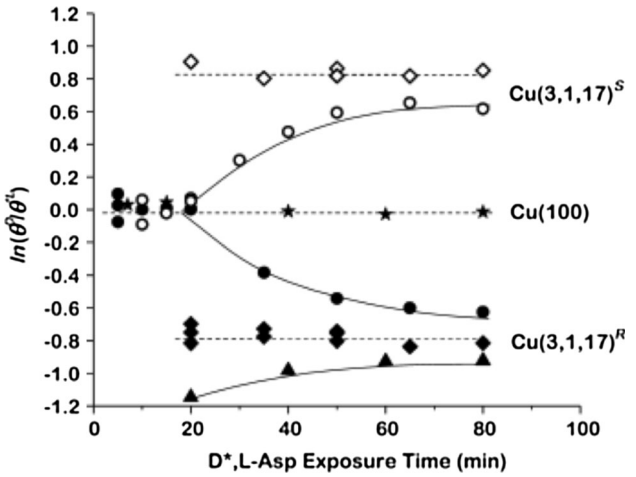

Fig. 3 Aspartic acid (Asp) coverage ratios, $\ln(\theta^{D}/\theta^{*L})$, on $Cu(3,1,17)^{R\&S}$ and on Cu(100), at 460 K as a function of exposure time to racemic D*L-Asp (the asterisk denote isotope labeling in the L-Asp enantiomer). No enantioselective enhancement is seen in the control experiment on the achiral Cu(100) surface ($\theta^{D}/\theta^{*L} = 1.0$, *star*), but, on the $Cu(3,1,17)^{R}$ surface, the coverage ratio evolves towards $\theta^{D}/\theta^{*L} = 0.46$ regardless of the initial value (1.0, *filled circle*; 0.32, *filled triangle*; and 0.46 *filled diamond*), and on the $Cu(3,1,17)^{S}$ surface the coverage ratio tends towards $\theta^{D}/\theta^{*L} = 2.3$ (initial coverage ratios: 1.0, *opened circle*; and 2.3, *opened diamond*). Reproduced from Ref. [31, Fig. 5] with permission, Copyright 2013 Wiley–VCH Verlag GmbH & Co.

enantiospecific differences in the adsorption energies of *R*- and *S*-3-MCHO at the kinks of $Cu(643)^{R\&S}$ surfaces [27]. Using a much more sophisticated ^{13}C isotope labeling methodology in TPD experiments, evidence for such enantioselective equilibrium separation starting with a racemic mixture of D- and *L-aspartic acid on naturally chiral $Cu(3,1,17)^{R\&S}$ surface was recently reported by Gellman et al. (Fig. 3) [31]. Equilibrium constant ratios between homochiral and heterochiral adsorbate–surface pairs of 2.2 ± 0.2 were estimated to translate into a Gibbs free energy difference of $\Delta(\Delta G) = 3.3 \pm 0.3$ kJ/mole. Interestingly, in a separate set of experiments, auto-amplification of enantiomeric excess (ee) in adsorbed aspartic acid was observed during adsorption of non-racemic mixtures on an achiral Cu(111) surface. Measurements of this phenomenon over a range of ee values in the gas mixture revealed a non-linear effect on the ee of the adsorbed layer, an observation that offers the potential for the development of enantioselective separation protocols exploiting this property but on achiral surfaces.

An alternative amplification effect applicable to enantioseparations is that relying on non-linear kinetics. This possibility has been recently illustrated in the Gellman laboratory for the decomposition of *R*,*R*- and *S*,*S*-tartaric acid on Cu single-crystal chiral surfaces. Their decomposition occurs by a surface explosion mechanism with highly non-linear kinetics resulting from a vacancy-mediated mechanism. This mechanism was shown to lead to highly enantiospecific decomposition rates that differ by as much as 2 orders of magnitude despite the fact that the effective rates constants for decomposition differ by less than a factor of 2 (Fig. 4) [32, 33].

The kink sites on chiral single-crystal surfaces have also been shown to be dynamic in nature [34, 35]. Clean chiral surfaces such as those shown in Figs. 1a and 4 are prone to thermal roughening in which atoms diffuse along step edges and result in coalescence of the kinks. In spite of this thermal roughening these surfaces retain their net chirality. An interesting consequence of this behavior is that even achiral surfaces may show chiral kinks at a local level, although on average a racemic mixture of *R*- and *S*-kinks is formed on the surface at a macroscopic level. The adsorption of chiral molecules on surfaces can further complicate the dynamic changes in surface structure. They can cause straight step edges to form chiral kinks, flat low Miller index surfaces to facet into chiral high Miller index planes, and the extraction of atoms from an achiral surface to form chiral arrays of adatoms. This adsorbate-induced restructuring of solid surfaces can be used to "imprint" new chiral structures into surfaces that are initially achiral [36–39]. For instance, recent scanning tunneling microscopy (STM) images have revealed that adsorbed tartaric acid extracts Cu atoms from an achiral Cu(110) surface to form highly ordered, chiral adatom arrays capped by a continuous molecular layer [40]. In some instances, these homochiral domains, made on achiral surfaces, may extend over reasonably large distances.

3 Chirally Templated Surfaces

On surfaces that are not intrinsically chiral, enantioselectivity may be imparted via the adsorption of chiral molecules. This new chirality can be provided entirely by the molecular structure of the individual molecules bonded to the surface, as discussed in the next section, but can also be created as a result of the formation of supramolecular structures on the surface. This latter modality is particularly important in cases where the added chiral modifiers are small or simple molecules not capable of directing enantioselective surface pathways on their own.

Chiral molecules adsorbed on single-crystal metal surfaces have been shown to form complex two-dimensional structures, many with specific enantiomeric characteristics [41, 42]. In fact, because surfaces lower the symmetry of adsorbates, chiral molecules can display more complex behavior on surfaces than in gas or liquid phase, and so-called prochiral molecules, which are not chiral in their isolated state but can become chiral upon adsorption, are also capable of forming ordered structures with enantiospecific characteristics [43, 44]. The idea that these

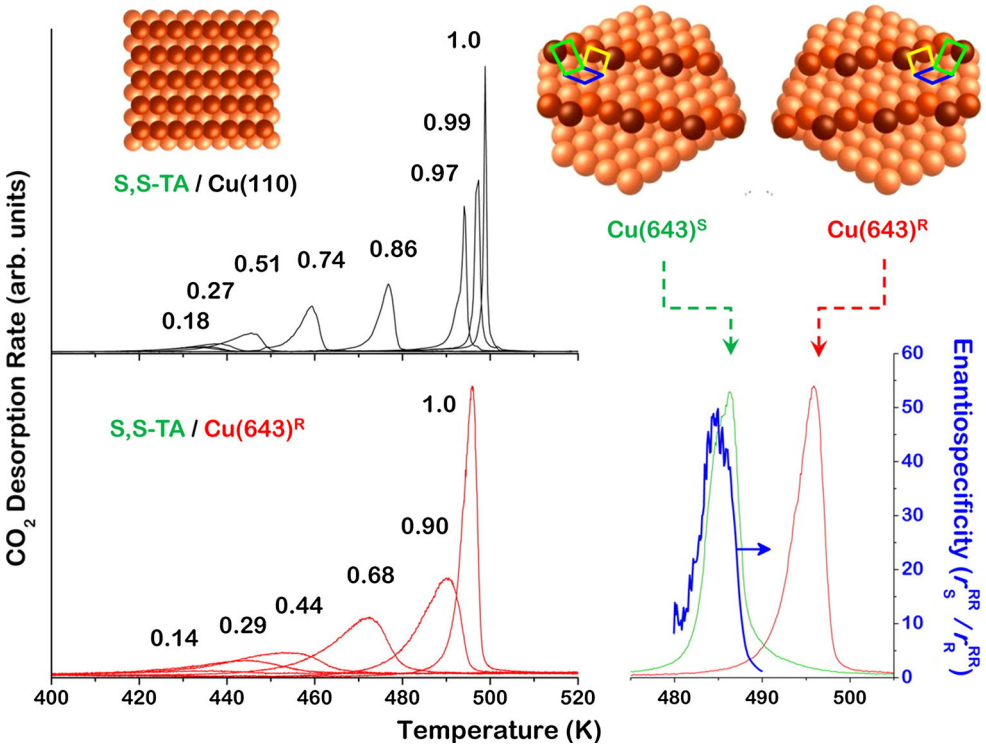

Fig. 4 CO_2 TPD traces from decomposition of *S,S*-tartaric acid (*S,S*-TA) on Cu(110) (*upper left*) and $Cu(643)^{R\&S}$ (*lower left*) surfaces as a function of initial coverage, as indicated on the figure. The large peak shifts and narrow peak widths seen here are signatures of a vacancy-mediated explosive decomposition mechanism. *Upper right* Enantiomorphic structures of the chiral $Cu(643)^{R\&S}$ surfaces. *Lower right* Contrasting TPD from saturation layers of *S,S*-TA on $Cu(643)^{R}$ (*red trace*) versus $Cu(643)^{S}$ (*green*) surfaces revealing enantiospecific decomposition kinetics, with the ratio of the reaction rates (*blue*) reaching a maximum of 50 at T = 485 K. Reproduced from Ref. [33, Fig. 1] with permission, Copyright 2013 The American Chemical Society

supramolecular chiral structures on surfaces may bestow enantioselectivity to achiral surfaces was first introduced by Wells and coworkers [45], but it is thanks to chiral titration experiments devised by the group of Tysoe to measure enantioselectivity of chiral overlayers in UHV that this possibility can be tested experimentally [46].

In their initial experiments, the ability of 2-butoxide species to create chiral adsorption pockets on a Pd(111) single-crystal surface was tested by using enantiopure propylene oxide as a probe molecule and TPD and reflection absorption infrared spectroscopy (RAIRS) to examine the differences in propylene oxide uptake in homochiral versus heterochiral pairings with 2-butoxide (Fig. 5) [46]. It was found that there is an enantioselective effect in propylene oxide (PO) uptake of as much as a factor of two between the homochiral and heterochiral pairs of templating agent and probe molecule for a coverage of approximately 25 % of monolayer saturation of the 2-butoxide. Interestingly, the enantioselectivity effect is only observed for intermediate 2-butoxide coverages, and disappears as more 2-butanol is adsorbed on the surface, an effect that has been explained, using Monte Carlo simulations, via a requirement of the formation of specific supramolecular ensembles on the surface [47]. Further refinements also revealed that enantioselective chemisorption is only found when 2-butanol rather than 2-butoxide is present on the surface, an observation that has been ascribed to enantiospecific hydrogen-bonding interactions between 2-butanol and PO [48].

The chiral supramolecular templating effect has since been observed with other templating molecules (2-methylbutanoate and 2-aminobutanoate species [9]), with other templating/probe pairs (proline/2-butanol [49] and 1-(1-naphthyl)ethylamine (NEA)/2-butanol [50]), and on other surfaces, including Au/Pd(111) [51], Pt(111) (with 2-butanol [52], 2-methyl butanoic acid [53], and NEA [54] as templating molecules), and Cu(100) (with a PO/lysine probe/template pair [55]). On the other hand, no enantioselectivity could be detected with PO on alanine-modified Cu(110), PO on alaninol-modified Cu(111), PO on 2-butanol-modified Cu(111), PO on 2-butoxide-modified Cu(100), PO on 2-butoxide-modified Cu(111), *R*-3-MCHO on 2-butoxide-modified Cu(100), or *R*-3-MCHO on 2-butoxide-modified Cu(111) [56]. These differences have been tentatively explained on the basis of possible hydrogen bonding among adsorbates, but more studies are required to develop a definitive answer to the question of what makes chiral templating work in some cases but not in others.

The role of hydrogen bonding in this chiral templating chemistry has been explored in more detail by the group of Tysoe and coworkers by looking into the details of possible deprotonation steps and zwitterion formation on surfaces. It was found that, in the case of tartaric acid (TA) on Pd(111), deprotonation of the carboxylic groups happens readily at room temperature. Accordingly, the lack of enantioselectivity in PO uptake on the TA-modified surface may be justified by the inability of the hydrogen-bonding proton acceptor site in PO to bind to the –OH groups on TA [57].

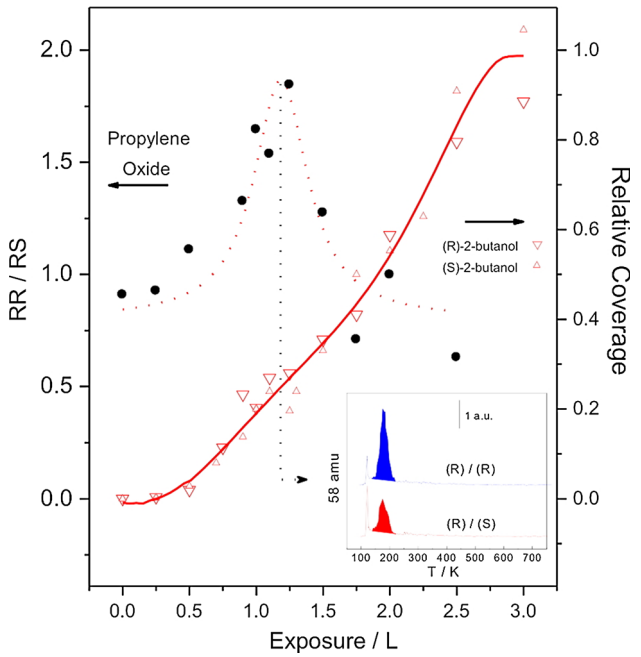

Fig. 5 Relative coverage of *S*-2-butoxide (*upward pointing triangles*) and *R*-2-butoxide (*downward pointing triangles*) on Pd(111) (*right axis*), and ratio of the coverage of *R*-propylene oxide (*R*-PO) adsorbed on *R*-2-butoxide-covered Pd(111) (RR) to the saturation coverage of *R*-PO adsorbed on *S*-2-butoxide (RR/RS) (*filled black circles*) (*left axis*), both as a function of 2-butanol exposure. *Inset* typical desorption spectra of *R*-PO from *R*- and *S*-2-butoxide-covered Pd(111). Reproduced from Ref. [46, Fig. 6] with permission, Copyright 2002 The American Chemical Society

Other chiral probes are being tested at the present time to corroborate this hypothesis.

Another important issue related to the chiral templating of surfaces is that of the interactions of the templating molecules among themselves when adsorbed on the surface, since those may control the final structure of the chiral supramolecular ensembles that define the enantiospecific adsorption pockets on the surface. In the case of aminoacids, the adsorbed molecules have shown their ability to form dimers, tetramers, and other clustering structures, and the nature of those structures appears to influence their ability to chirally template the metal surface. In initial experiments from the Tysoe group with alanine on Pd(111), adsorption at 290 K was shown to result in both anionic and zwitterionic species. However, DFT calculations showed that zwitterionic aminoacids are much less stable on surfaces than the anions [58] due to the stronger binding of NH_2 than NH_3^+ groups. It was found that the zwitterion is stabilized by forming a dimer with an anionic species by interaction with the carboxylate group of the anion. These stable dimeric units constitute the basis for the formation of more complex structures. For example, dimer rows form by assembling from parallel anionic–zwitterionic species. In addition, tetramers form from assembly of two antiparallel dimers in which three of the alanine molecules undergo a concerted rotation by 30° to form a more stable structure (Fig. 6) [59]. Preliminary studies with this and other aminoacids have suggested that enantioselectivity in the uptake of PO is seen only for templating agents that form tetramers. The chiral pocket formed at the center of the tetrameric unit provides an attractive candidate as a chiral template, and this idea is currently being explored by the Tysoe group.

The intermolecular interactions among adsorbed templating molecules are particularly critical in cases where there may be differences between enantiopure versus mixed-enantiomeric layers. In connection with this, interesting symmetry breaking has been reported in some cases, induced either by chiral seeding [60–62], or via amplification of small imbalances in enantiomeric composition [41, 63, 64]. Zaera and coworkers have recently identified kinetic differences in the uptake of PO on Pt(111) surfaces depending on the composition of both adsorbed and gas-phase mixtures [65, 66]. Specifically, the saturated monolayer of a racemic (50:50) mixture was found to be approximately 20 % less dense than a similar enantiopure layer of PO, and the sticking coefficient was seen to increase initially with surface coverage and to yield different values for homo- versus hetero-chiral pairs of PO in the gas phase versus the surface. A combination of TPD, STM, molecular beam experiments, and kinetic Monte Carlo simulations were used to determine that the origin of this behavior is adsorbate-assisted kinetics for the adsorption of PO, with different adsorption probabilities for homo- versus hetero-enantiomeric pairs (Fig. 7) [65].

In a separate study, RAIRS spectra of saturated monolayers of racemic NEA adsorbed from CCl_4 solutions onto Pt surfaces were shown to differ from those of enantiopure monolayers, a behavior that was proposed to result from the formation of racemate pairs via hydrogen bonding at the amine moiety also responsible for bonding to the surface [54, 66]. The effect of these differences on the ability of such chiral modifiers to generate chiral adsorption sites on metal surfaces is to be explored next.

4 One-to-One Chiral Modifiers

When the chiral modifier is relatively large, it may be possible for individual molecules to provide the chiral environment on the surface required to bestow enantioselectivity to the catalysts without the need to form chiral supramolecular ensembles. This is believed to be the case in the so-called Orito reaction, the enantioselective hydrogenation of α-ketoesters catalyzed by platinum-based catalysts modified by chiral cinchona alkaloids. This reaction has been studied extensively and many aspects of

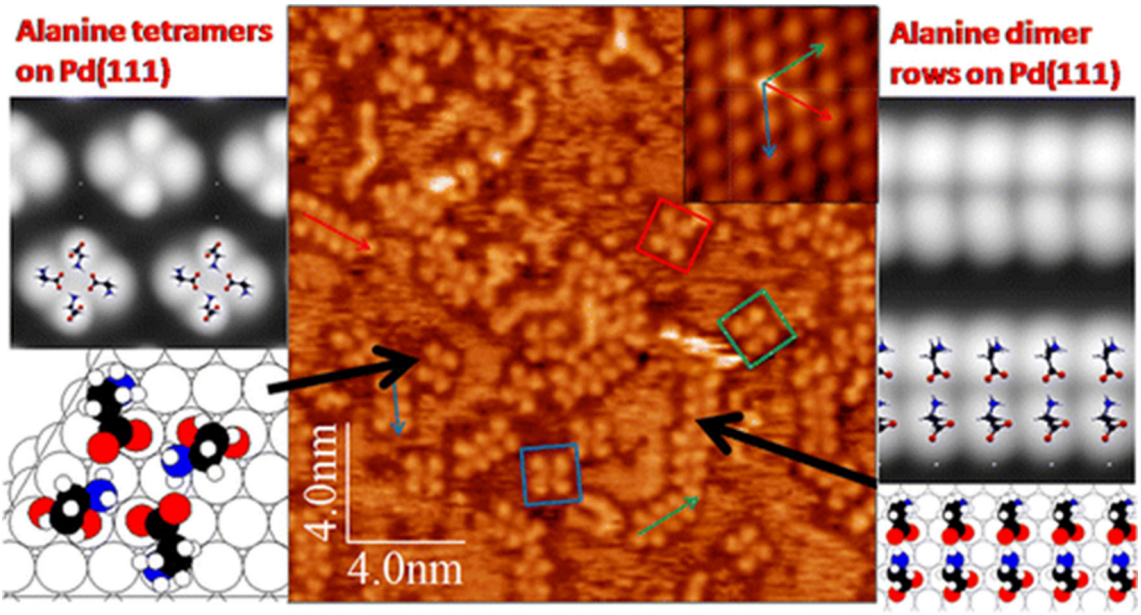

Fig. 6 *Center* Scanning tunneling microscopy (STM) image of alanine adsorbed on Pd(111) at 290 K. The *inset* corresponds to an image of the clean Pd(111) surface, provided as reference. The *squares* highlight three arbitrarily chosen tetramers used to follow their motion. *Sides* Simulated STM images for the tetramers (*left*) and dimer rows (*right*) identified in the experimental data. Reproduced from Ref. [59, Graphical Abstract] with permission, Copyright 2014 The American Chemical Society

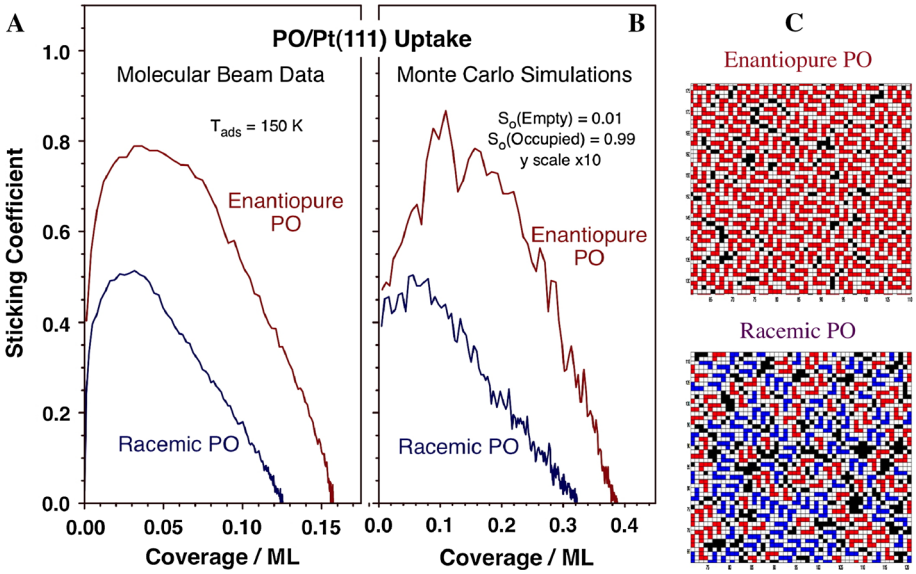

Fig. 7 Experimental (**a**) and Monte Carlo-simulated (**b**) isothermal uptake curves for enantiopure (*red*) and racemic (*blue*) PO on Pt(111). Higher saturation coverages and sticking coefficients are always seen with the enantiopure molecules compared to the racemic PO, and an initial increase in sticking coefficient is also observed because of the adsorbate-assisted nature of the sticking process. **c** Snapshots of the simulated surfaces obtained at saturation with enantiopure (*top*) and racemic (*bottom*) PO. Reproduced from Ref. [65, Fig. 4] with permission, Copyright 2013 The American Chemical Society

the process have been explained, but many questions remain still [6, 8, 67–70]. Moreover, it has not been possible to extend the process to a broad range of reactions or reactants. Nevertheless, a general picture has emerged in which the cinchona modifier forms a weakly bonded complex with the α-ketoester around its chiral center, forcing adsorption of the carbonyl group of the reactant preferentially into one of its two possible orientations [71–73].

In the past, the Zaera group has contributed to the molecular understanding of this system by using RAIRS to study the details of the cinchona alkaloid adsorption on

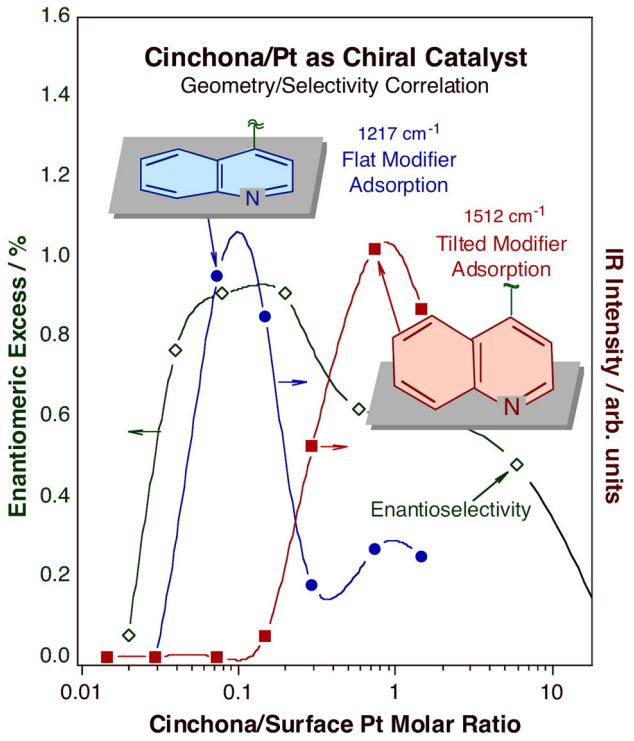

Fig. 8 Correlation between the adsorption geometry of cinchonidine (Cd) adsorbed from solution (in CCl_4) onto a Pt surface, measured by in situ RAIRS, and the selectivity of the catalytic enantioselective hydrogenation of ethyl pyruvate by a Cd-modified platinum catalyst [127]. A maximum in enantioselectivity is observed for intermediate Cd concentrations, for which the adsorbed modifier adopts a flat-lying geometry. Counterintuitively, higher concentrations of the modifier lead to a deterioration in catalytic performance. The RAIRS data indicate that this is because the quinoline ring of the modifier tilts on the surface to accommodate the ensuing higher coverages; that removes the chiral pocket of the cinchona away from the surface. Reproduced from Ref. [128, Fig. 6] with permission, Copyright 2014 The Royal Society of Chemistry

platinum surfaces in situ at the liquid–solid interface [10, 11, 74, 75]. The first main conclusion resulting from that work was that the performance of the cinchona/platinum system is optimized by a flat-lying adsorption geometry of the aromatic ring of the cinchona modifier, which the molecule adopts only within a narrow intermediate range of concentrations in solutions (Fig. 8) [76–78]. Additional experiments provided further insight into the effects on cinchona adsorption exerted by structural modifications to the modifier [75], in particular by changing its peripheral groups [78], and also by the choice of solvent [74, 79, 80], by protonation in an acidic environment [81], and by the addition of gases to the solution [74, 82]. Estimates were obtained for the adsorption constants of many cinchona alkaloids and related compounds [10, 83]. Lastly, a physicochemical analysis of the competitive adsorption of pairs of these chiral adsorbates was carried out to understand their relative ability for chiral modification of surfaces in terms of both adsorption equilibria and solubility [10, 11, 84].

Given that ultrahigh-vacuum (UHV) surface analysis studies with cinchona alkaloids are difficult, much research has been carried out with a simpler representative of such chiral modifiers, 1-(1-naphthyl)ethylamine (NEA). Even though NEA has a much smaller chiral group than the cinchona alkaloids, it has been shown to bestow moderate enantioselectivity to platinum catalysts [70, 85, 86]. Indeed, NEA contains the main functionalities believed to be responsible for the modifying behavior of the cinchona alkaloids, namely, an aromatic ring and an amine group near a chiral center [8, 87]. Based on surface-science studies under UHV [88–90], adsorption of the modifier on the metal has been proposed to occur through the aromatic ring. Extensive work by McBreen and coworkers, mainly relying on surface imaging using STM but also using vibrational spectroscopies, have provided nice experimental evidence for the formation of hydrogen-bonded complexes between NEA and a number of model reactants on platinum single-crystal surfaces [91–100].

The research groups of Tysoe and Zaera both have studied the adsorption of NEA, on Pd(111) [50, 101, 102] and Pt(111) and polycrystalline Pt [10, 47, 54, 66, 103] surfaces, respectively, and have acquired evidence supporting a basic understanding of the NEA chiral chemistry. Specifically, Tysoe and coworkers reported STM data [102] and density functional theory (DFT) calculations [101] pointing to the adsorption of NEA in two different conformations, *endo* and *exo*, which are likely to interact differently with the reactant (Fig. 9). TPD, STM, and RAIRS evidence was also obtained for hydrogen bonding between NEA and 2-butanol [50]. On Pt(111), Zaera showed that NEA bestows enantioselectivity only at intermediate coverages, as expected from modifiers that form chiral supramolecular templates (as discussed above). However, it also displays different interaction energetics with the two enantiomers of PO, indicative of the participation of a one-to-one modifier-reactant (or probe molecule) interaction in this chemistry [10, 47, 54]. It should be indicated that no evidence of NEA templating was seen on Pd(111) [102], suggesting that the nature of the surface also plays a role in the mechanism of enantioselective surface chemistry discussed in this Perspective. Additional, in situ RAIRS studies of NEA adsorption at the solid–liquid interface highlighted the critical role that the solvent plays in defining the nature of the adsorbed NEA species [54, 66, 74], even suggesting that the key interaction with the surface may involve the amine group rather than the aromatic ring, as commonly believed (Fig. 10) [103].

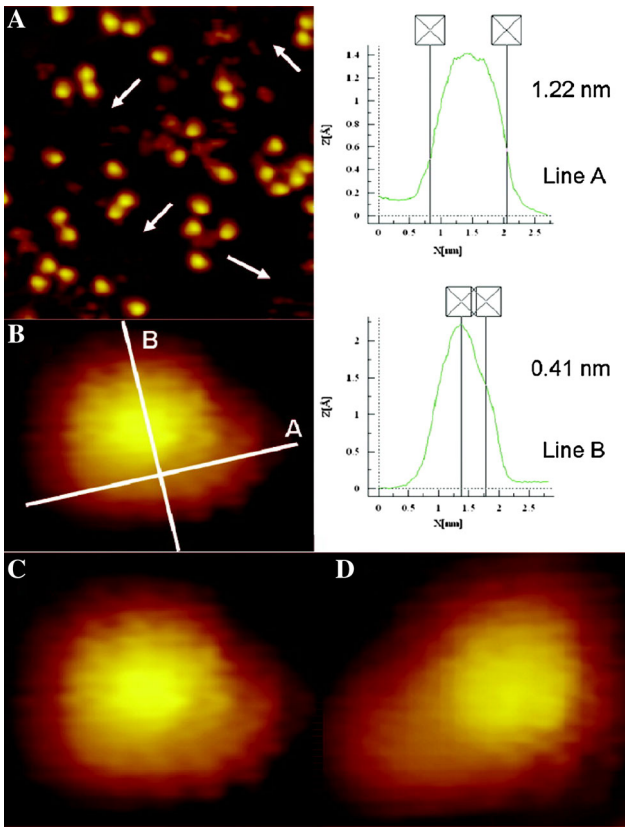

Fig. 9 STM images of NEA adsorbed on Pd(111) at 100 K. **a** Low (20.1 nm × 20.1 nm) resolution image. **b** High resolution image of an individual adsorbate. The profiles along the *white lines* (*A* and *B*) are shown on the *right*. **c**, **d** Additional individual images illustrating the two different conformations, *exo* and *endo*, identified for NEA on the Pd(111) surface. Reproduced from Ref. [102, Fig. 1] with permission, Copyright 2011 The American Chemical Society

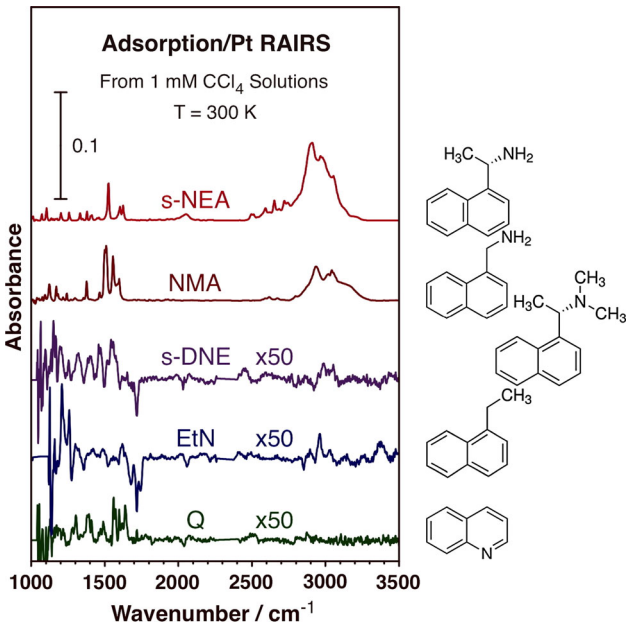

Fig. 10 Comparative RAIRS data from s-NEA and related compounds adsorbed from CCl_4 solutions on a Pt polycrystalline surface. The experiments were designed to identify the moiety responsible for bonding to the surface. Extensive uptake is only seen with NEA and 1-naphthylmethylamine (NMA), not with (*S*)-(–)-*N*,*N*-dimethyl-1-(1-naphthyl)ethylamine (s-DNE), 1-ethylnaphthalene (EtN), or quinoline (Q), indicating that it is the amine and not the aromatic ring that facilitates the adsorption. Reproduced from Ref. [103, Fig. 1] with permission, Copyright 2013 Wiley–VCH Verlag GmbH & Co.

5 Studies with More Realistic Catalyst Models

The majority of the studies described above were carried out with small-area planar metal surfaces, typically using single crystals, and under controlled conditions, in many instances in vacuum. In some instances, our groups have also expanded this research to test enantioselective surface chemistry on nanoparticles and other more realistic catalytic samples. In one case, the enantioselectivity of the adsorption of chiral molecules on gold nanoparticles chirally modified with either D- or L-cysteine, to render them chiral, was probed by optical rotation measurements [104]. Some work has already been published by others on chiral metal nanoparticles, but those studies have focused on structural and physical properties [105–107]. In Shukla's work, it was found that the chirally modified Au nanoparticles selectively adsorb one enantiomer of PO from a racemic solution, thus leaving an enantiomeric excess in the liquid phase (Fig. 11). A simple adsorption model was developed for the quantitative determination of the ratios of the enantiospecific adsorption equilibrium constants in these systems directly from optical rotation measurements [108].

The Zaera group has also explored the possibility of using self-assembled monolayers as a way to improve the performance of Pt nanoparticles for the Orito reaction [109]. They found that the addition of alkyl thiol self-assembled monolayers (SAMs) to colloidal platinum nanoparticles suspended in the liquid phase leads to significant improvements in both activity and enantioselectivity in the hydrogenation of ethyl pyruvate modified via the addition of cinchonidine to the solution (compared to those seen with naked Pt nanoparticles). This may be explained by an increase in cinchonidine residence time on the surface. Those cases involved both Pt nanoparticles and the cinchona alkaloid in solution, but even though more nuanced compromises between activity and selectivity were identified when using supported catalysts, reasonable performances were still found to be possible with all-heterogeneous Pt/Al_2O_3 catalysts covered with thiol-tethered cinchonidine SAMs.

Chiral modification can also be attained by tethering chiral molecules to the high-surface-area porous materials often used as supports in heterogeneous catalysts. The tethering, anchoring, or immobilization of homogeneous

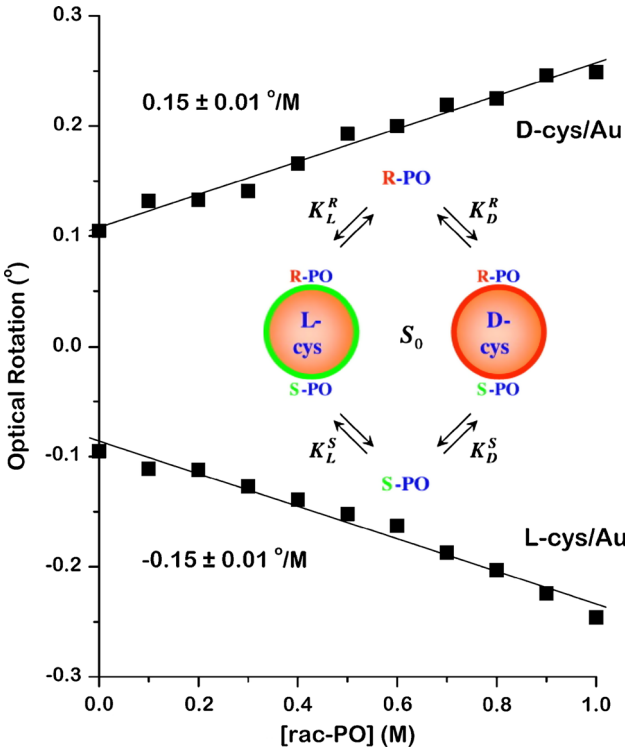

Fig. 11 Rotation of polarized light by racemic PO added to solutions containing Au nanoparticles modified with either L- or D-cysteine. The data show that PO interacts enantiospecifically with the chirally-modified Au nanoparticles, thus causing an increase in rotation of polarized light with increasing racemic PO concentration. This behavior can be accounted for by differences in the enantiospecific equilibrium constants shown schematically in the *inset*. Adapted from Refs. [104, Fig. 3] and [108, Fig. 1] with permissions, Copyright 2010 The American Chemical Society and 2014 Elsevier

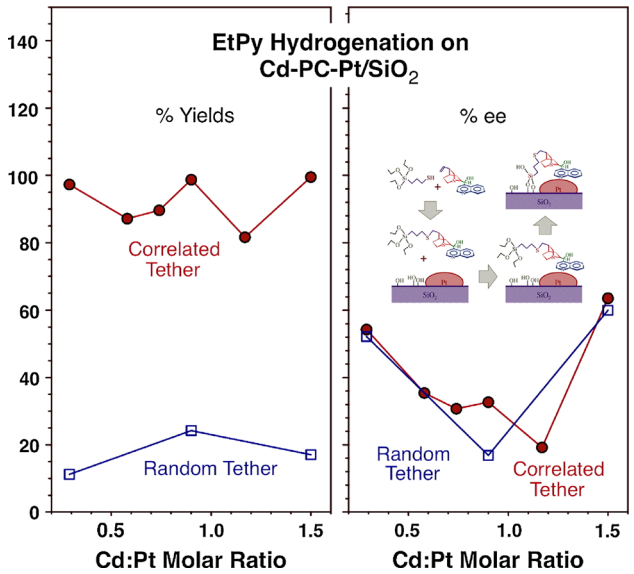

Fig. 12 Total yields (*left frame*) and ee's (*right*) after a 6 h hydrogenation reaction of ethyl pyruvate in acetic acid using cinchonidine-modified Pt/SiO_2 catalysts as a function of Cd:Pt molar ratio. Data are contrasted for samples where the Cd was tethered on the silica surface in random versus correlated fashion. A clear improvement in catalytic performance, mainly in total activity but also in ee (in some cases), is seen with the latter. *Inset* Schematic depiction of the strategy used to prepare the correlated tethered catalyst. Reproduced from Ref. [120, Fig. 10 and graphical abstract] with permission, Copyright 2014 The Royal Society of Chemistry

organometallic catalysts, including compounds capable of promoting enantioselectivity, has been extensively explored in the past [110–113], and will not be reviewed here. Alternatively, molecular functionality, chiral or otherwise, can be added to porous solids by using so-called "click" chemistry, via the use of an intermediate linking agent [110, 113, 114]. Bestowing enantioselectivity onto a high-surface-area silica catalyst by tethering cinchonidine with propyltriethoxysilane as the linker was successful for the addition of aromatic thiols to unsaturated ketones, a reaction promoted by amines (the tertiary quinuclidine nitrogen atom in the case of cinchonidine) [115]. However, a loss of enantioselectivity was observed upon tethering, which could be accounted for by a combination of at least three effects: (1) the nonselective catalytic activity of the surface of the solid itself; (2) the activity of the OH species generated by hydrolysis of some of the Si-alkoxy groups in the trialkoxy moieties used to bind many linkers to oxide surfaces; and (3) the bonding of the molecule to be tethered directly to the surface [116]. These problems could be minimized by silylation of the active OH groups on the surface of the oxide support, and by a proper selection of linking position within the cinchonidine and the solvent used.

Finally, the Zaera group has recently explored the possibility of adding enantioselectivity to supported Pt catalysts used for the Orito reaction via the tethering of cinchonidine to the surface of the supporting oxide in those catalysts. This idea has been tested by others in the past [117–119], but here a new methodology was advanced to perform the cinchonidine tethering in a correlated fashion, that is, selectively on sites adjacent to the Pt nanoparticles, in order to enhance the performance of the catalyst (Fig. 12) [120]. The protocol relies on the selective strong adsorption of the cinchona alkaloid on the platinum surface, the same interaction responsible for the chiral modification: a cinchonidine molecule to which a propyltriethoxysilane moiety has been added is first exposed to the catalyst, the excess is then washed away with pure solvent, and the click chemistry that links the chiral modifier to the surface of the silica surface is finally triggered via thermal activation. Superior performance, close to what is obtained with cinchonidine in solution, was seen with the correlated-tethering samples, manly in terms of activity but also with respect to enantioselectivity, when contrasted with similar samples with randomly-distributed tethered cinchonidine (Fig. 12).

6 Closing Remarks

As already mentioned in the introduction, enantioselective catalysis is of critical importance for the industrial production of many bioreactive compounds, and offers an interesting challenge in terms of the development of a basic molecular-level understanding of the issues that control selectivity in heterogeneous catalysis. Because heterogeneous catalysts are quite complex, modern surface scientists have taken the approach of investigating specific aspects of the chemistry involved, including the chemical adsorption of the relevant compounds on solid surfaces, by using model systems and controlled environments [121–123]. This Perspective of our work on chiral surface chemistry provides a good example of the advantages of such approach, and illustrates the level of knowledge that can be acquired on the mechanistic details of catalytic selectivity. At the same time, it also highlights its shortcomings, both in terms of the limited amount of information that can be extracted, even when using state-of-the-art surface sensitive analytical techniques, and in the difficulties that may be encountered in trying to extrapolate the information from model systems to realistic catalysts [124–126].

Clearly, much more work is needed before reaching the point of being able to design enantioselective catalysts based on the mechanistic lessons derived from fundamental research such as ours. Nevertheless, several useful conclusions have already been extracted from the work done so far. First, convincing evidence is now available for the existence of chiral surfaces, even in materials that are not intrinsically chiral as is the case with the transition metals reviewed here. Furthermore, it is also clear that those chiral surfaces can drive enantioselective chemistry, both in terms of adsorption–desorption phenomena and in connection with chemical transformations. The differences in behavior between pairs of enantiomers are typically small, with energetics that differ over a range of only a few kcal/mole at the most, but those are still sufficient to design enantioseparation and enantiodifferentiation processes under appropriate kinetic conditions. Furthermore, these small differences can be amplified into high enantiospecificity by processes, such as surface explosion reactions, with highly non-linear kinetics. These ideas have been proven with model surfaces, but still await extension to more realistic systems.

It has also been shown that achiral surfaces can be modified via the adsorption of chiral molecules to bestow enantioselectivity to catalytic systems. This chiral modification may originate entirely (or mainly) from interactions between the reactant and individual chiral molecules, but it is also feasible with small modifiers because of the possibility of the formation of supramolecular surface ensembles exhibiting chiral adsorption sites. The operation of both of these mechanisms and their impact on adsorption enantioselectivity have been clearly demonstrated by chiral titration experiments on model surfaces, and similar chemistry is likely to also explain the few catalytic examples where enantioselective modification has been achieved (although that remains to be conclusively demonstrated). Current work is aimed at achieving a better understanding of the chemistry between reactants and chiral modifiers, which appears to require hydrogen bonding but is most likely affected by other factors as well. The ultimate goal is to understand the processes imparting chirality to surfaces to the point of being able to identify and design new chiral catalytic systems. Much work remains to before reaching that goal.

Finally, some attempts have been initiated already to characterize more complex chiral systems, in the form of chirally modified metal nanoparticles and high-surface-area oxides. This work is only in its initial stages, but looks promising. We intend to continue this research, and hope to entice many other surface scientists to join us in this effort.

Acknowledgments Funding for the projects described in this Perspective has been provided mainly by the U. S. Department of Energy, Basic Energy Sciences, under Grant No. DE-FG02-12ER16330.

References

1. Zaera F (2002) J Phys Chem B 106:4043–4052
2. Somorjai GA, Park JY (2008) Angew Chem Int Ed 47:9212–9228
3. Zaera F (2012) Catal Lett 142:501–516
4. Blaser H-U, Pugin B, Spindler F (2005) J Mol Catal A 231:1–20
5. Thayer AM (2007) Chem Eng News 85:11–19
6. Y. Orito, S. Imai, S. Niwa, J Chem Soc Jpn (1980) 670–672
7. Osawa T, Harada T, Takayasu O (2006) Curr Org Chem 10:1513–1531
8. Mallat T, Orglmeister E, Baiker A (2007) Chem Rev 107:4863–4890
9. Stacchiola D, Burkholder L, Zheng T, Weinert M, Tysoe WT (2005) J Phys Chem B 109:851–856
10. Zaera F (2008) J Phys Chem C 112:16196–16203
11. Zaera F (2009) Acc Chem Res 42:1152–1160
12. Gellman AJ (2010) ACS Nano 4:5–10
13. Pratt SJ, Jenkins SJ, King DA (2005) Surf Sci 585:L159–L165
14. Horvath JD, Gellman AJ (2003) Top Catal 25:9–15
15. Sholl DS, Gellman AJ (2009) AIChE J 55:2484–2490
16. McFadden CF, Cremer PS, Gellman AJ (1996) Langmuir 12:2483–2487
17. Sholl DS (1998) Langmuir 14:862–867
18. Power TD, Sholl DS (1999) J Vac Sci Technol A 17:1700–1704
19. Ahmadi A, Attard G, Feliu J, Rodes A (1999) Langmuir 15:2420–2424
20. Attard GA, Ahmadi A, Feliu J, Rodes A, Herrero E, Blais S, Jerkiewicz G (1999) J Phys Chem B 103:1381–1385
21. Gellman AJ, Horvath JD, Buelow MT (2001) J Mol Catal A 167:3–11
22. Horvath JD, Gellman AJ (2001) J Am Chem Soc 123:7953–7954

23. Horvath JD, Gellman AJ (2002) J Am Chem Soc 124:2384–2392
24. Cheong WY, Gellman AJ (2010) J Phys Chem C 115:1031–1035
25. Rampulla DM, Gellman AJ (2006) Surf Sci 600:2823–2829
26. Rampulla DM, Francis AJ, Knight KS, Gellman AJ (2006) J Phys Chem B 110:10411–10420
27. Horvath JD, Koritnik A, Kamakoti P, Sholl DS, Gellman AJ (2004) J Am Chem Soc 126:14988–14994
28. Huang Y, Gellman A (2008) Catal Lett 125:177–182
29. Huang Y, Gellman A (2011) Top Catal 54:1403–1413
30. Horvath JD, Baker L, Gellman AJ (2008) J Phys Chem C 112:7637–7643
31. Yun Y, Gellman AJ (2013) Angew Chem Int Ed 52:3394–3397
32. Mhatre BS, Pushkarev V, Holsclaw B, Lawton TJ, Sykes ECH, Gellman AJ (2013) J Phys Chem C 117:7577–7588
33. Gellman AJ, Huang Y, Feng X, Pushkarev VV, Holsclaw B, Mhatre BS (2013) J Am Chem Soc 135:19208–19214
34. Baber AE, Gellman AJ, Sholl DS, Sykes ECH (2008) J Phys Chem C 112:11086–11089
35. Zhao X, Perry SS, Horvath JD, Gellman AJ (2004) Surf Sci 563:217–224
36. Zhao XY (2000) J Am Chem Soc 122:12584–12585
37. Zhao XY, Zhao RG, Yang WS (2000) Langmuir 16:9812–9818
38. Durán Pachón L, Yosef I, Markus TZ, Naaman R, Avnir D, Rothenberg G (2009) Nat Chem 1:160–164
39. Karageorgaki C, Ernst K-H (2014) Chem Comm 50:1814–1816
40. Lawton TJ, Pushkarev V, Wei D, Lucci FR, Sholl DS, Gellman AJ, Sykes ECH (2013) J Phys Chem C 117:22290–22297
41. Mark AG, Forster M, Raval R (2010) Tetrahedron Asymmetry 21:1125–1134
42. Ernst K-H (2012) Phys Status Solidi B 249:2057–2088
43. Mark AG, Forster M, Raval R (2011) ChemPhysChem 12:1474–1480
44. Ernst K-H (2013) Surf Sci 613:1–5
45. Sutherland IM, Ibbotson A, Moyes RB, Wells PB (1990) J Catal 125:77–88
46. Stacchiola D, Burkholder L, Tysoe WT (2002) J Am Chem Soc 124:8984–8989
47. Sales JL, Gargiulo V, Lee I, Zaera F, Zgrablich G (2010) Catal Today 158:186–196
48. Gao F, Wang Y, Burkholder L, Tysoe WT (2007) J Am Chem Soc 129:15240–15249
49. Gao F, Wang Y, Tysoe WT (2008) J Phys Chem C 112:6145–6150
50. Burkholder L, Stacchiola D, Boscoboinik JA, Tysoe WT (2009) J Phys Chem C 113:13877–13885
51. Gao F, Wang Y, Li Z, Furlong O, Tysoe WT (2008) J Phys Chem C 112:3362–3372
52. Lee I, Zaera F (2005) J Phys Chem B 109:12920–12926
53. Lee I, Zaera F (2006) J Am Chem Soc 128:8890–8898
54. Lee I, Ma Z, Kaneko S, Zaera F (2008) J Am Chem Soc 130:14597–14604
55. Cheong WY, Gellman AJ (2012) Langmuir 28:15251–15262
56. Cheong WY, Huang Y, Dangaria N, Gellman AJ (2010) Langmuir 26:16412–16423
57. Mahapatra M, Tysoe WT (2014) Surf Sci. doi:10.1016/j.susc.2014.1003.1001
58. James JN, Sholl DS (2008) J Mol Catal A 281:44–48
59. Mahapatra M, Burkholder L, Bai Y, Garvey M, Boscoboinik JA, Hirschmugl C, Tysoe WT (2014) J Phys Chem C 118:6856–6865
60. Parschau M, Romer S, Ernst K-H (2004) J Am Chem Soc 126:15398–15399
61. Roth C, Passerone D, Ernst KH (2010) Chem Commun 46:8645–8647
62. Ernst KH (2010) Origins Life Evol Biosph 40:41–50
63. Parschau M, Fasel R, Ernst K-H (2008) Cryst Growth Des 8:1890–1896
64. Haq S, Liu N, Humblot V, Jansen APJ, Raval R (2009) Nat Chem 1:409–414
65. Karakalos S, Lawton TJ, Lucci FR, Sykes ECH, Zaera F (2013) J Phys Chem C 117:18588–18594
66. Gordon AD, Karakalos S, Zaera F (2014) Surf Sci. doi:10.1016/j.susc.2014.1002.1003
67. Attard GA, Griffin KG, Jenkins DJ, Johnston P, Wells PB (2006) Catal Today 114:346–352
68. Blaser H-U, Studer M (2007) Acc Chem Res 40:1348–1356
69. Ma Z, Zaera F (2009) In: Ozkan US (ed) Design of heterogeneous catalysis: new approaches based on synthesis, characterization, and modelling. Wiley, Weinheim, pp 113–140
70. Tálas E, Margitfalvi JL (2010) Chirality 22:3–15
71. Vayner G, Houk KN, Sun Y-K (2004) J Am Chem Soc 126:199–203
72. Vargas A, Ferri D, Bonalumi N, Mallat T, Baiker A (2007) Angew Chem Int Ed 46:3905–3908
73. Schmidt E, Bucher C, Santarossa G, Mallat T, Gilmour R, Baiker A (2012) J Catal 289:238–248
74. Ma Z, Lee I, Kubota J, Zaera F (2004) J Mol Catal A 216:199–207
75. Mink L, Ma Z, Olsen RA, James JN, Sholl DS, Mueller LJ, Zaera F (2008) Top Catal 48:120–127
76. Kubota J, Zaera F (2001) J Am Chem Soc 123:11115–11116
77. Chu W, LeBlanc RJ, Williams CT, Kubota J, Zaera F (2003) J Phys Chem B 107:14365–14373
78. Lai J, Ma Z, Mink L, Mueller LJ, Zaera F (2009) J Phys Chem B 113:11696–11701
79. Ma Z, Zaera F (2005) J Phys Chem B 109:406–414
80. Zaera F (2005) Chem Rec 5:133–144
81. Olsen RA, Borchardt D, Mink L, Agarwal A, Mueller LJ, Zaera F (2006) J Am Chem Soc 128:15594–15595
82. Ma Z, Kubota J, Zaera F (2003) J Catal 219:404–416
83. Ma Z, Lee I, Zaera F (2007) J Am Chem Soc 129:16083–16090
84. Ma Z, Zaera F (2006) J Am Chem Soc 128:16414–16415
85. Heinz T, Wang G, Pfaltz A, Minder B, Schuerch M, Mallat T, Baiker A (1995) J Chem Soc Chem Commun 1421–1422
86. Orglmeister E, Mallat T, Baiker A (2005) Adv Synth Catal 347:78–86
87. Diezi S, Hess M, Orglmeister E, Mallat T, Baiker A (2005) J Mol Catal A 239:49–56
88. Stephenson MJ, Lambert RM (2001) J Phys Chem B 105:12832–12838
89. Bonello JM, Williams FJ, Lambert RM (2003) J Am Chem Soc 125:2723–2729
90. Lavoie S, Laliberté M-A, McBreen PH (2003) J Am Chem Soc 125:15756–15757
91. Lavoie S, Laliberté M-A, McBreen P (2004) Catal Lett 97:111–114
92. Lavoie S, Laliberte MA, Temprano I, McBreen PH (2006) J Am Chem Soc 128:7588–7593
93. Demers-Carpentier V, McBreen PH (2011) J Phys Chem C 115:6513–6520
94. Demers-Carpentier V, Goubert G, Masini F, Lafleur-Lambert R, Dong Y, Lavoie S, Mahieu G, Boukouvalas J, Gao H, Rasmussen AMH, Ferrighi L, Pan Y, Hammer B, McBreen PH (2011) Science 334:776–780
95. Goubert G, Demers-Carpentier V, Masini F, Dong Y, Lemay JC, McBreen PH (2011) Chem Comm 47:9113–9115
96. Brunelle J, Demers-Carpentier V, Lafleur-Lambert R, Mahieu G, Goubert G, Lavoie S, McBreen P (2011) Top Catal 54:1334–1339

97. Demers-Carpentier V, Goubert G, Masini F, Dong Y, Rasmussen AMH, Hammer B, McBreen PH (2012) J Phys Chem Lett 3:92–96
98. Demers-Carpentier V, Rasmussen AMH, Goubert G, Ferrighi L, Dong Y, Lemay J-C, Masini F, Zeng Y, Hammer B, McBreen PH (2013) J Am Chem Soc 135:9999–10002
99. Goubert G, McBreen PH (2014) ACS Catal 4:847–854
100. Groves MN, Goubert G, Rasmussen AMH, Dong Y, Lemay JC, Demers-Carpentier V, McBreen PH, Hammer B (2014) Surf Sci. doi:10.1016/j.susc.2014.1003.1008
101. Burkholder L, Garvey M, Weinert M, Tysoe WT (2011) J Phys Chem C 115:8790–8797
102. Boscoboinik JA, Bai Y, Burkholder L, Tysoe WT (2011) J Phys Chem C 115:16488–16494
103. Gordon AD, Zaera F (2013) Angew Chem Int Ed 52:3453–3456
104. Shukla N, Bartel MA, Gellman AJ (2010) J Am Chem Soc 132:8575–8580
105. Yao H (2008) Curr Nanosci 4:92–97
106. Noguez C, Garzon IL (2009) Chem Soc Rev 38:757–771
107. Gautier C, Bürgi T (2009) ChemPhysChem 10:483–492
108. Shukla N, Ondeck N, Gellman AJ (2014) Surf Sci. doi:10.1016/j.susc.2014.1003.1011
109. Weng Z, Zaera F (2014) J Phys Chem C 118:3672–3679
110. Corma A, Garcia H (2006) Adv Synth Catal 348:1391–1412
111. Heitbaum M, Glorius F, Escher I (2006) Angew Chem Int Ed 45:4732–4762
112. Copéret C, Basset J-M (2007) Adv Synth Catal 349:78–92
113. Pugin B, Blaser HU (2010) Top Catal 53:953–962
114. Margelefsky EL, Zeidan RK, Davis ME (2008) Chem Soc Rev 37:1118–1126
115. Hong J, Lee I, Zaera F (2011) Top Catal 54:1340–1347
116. Hong J, Zaera F (2012) J Am Chem Soc 134:13056–13065
117. Blaser H-U, Jalett H-P, Müller M, Studer M (1997) Catal Today 37:441–463
118. Huang Y, Xu S, Lin VSY (2011) ChemCatChem 3:690–694
119. Azmat MU, Guo Y, Guo Y, Wang Y, Lu G (2011) J Mol Catal A 336:42–50
120. Hong J, Lee I, Zaera F (2014) Catal Sci Technol. doi:10.1039/c4cy00844h
121. Somorjai GA (1994) Introduction to surface chemistry and catalysis. Wiley, New York
122. Zaera F (2001) Prog Surf Sci 69:1–98
123. Ertl G (2008) Angew Chem Int Ed 47:3524–3535
124. Ma Z, Zaera F (2006) Surf Sci Rep 61:229–281
125. Freund HJ (2010) Chem Eur J 16:9384–9397
126. Gao F, Goodman DW (2012) Annu Rev Phys Chem 63:265–286
127. LeBlond C, Wang J, Liu J, Andrews AT, Sun Y-K (1999) J Am Chem Soc 121:4920–4921
128. Zaera F (2014) Chem Soc Rev. doi:10.1039/C1033CS60374A